

Gravitational Lensing Effects on the Baryonic Acoustic Oscillation Signature in the Redshift-Space Correlation Function

Jaiyul Yoo^{1*} and Jordi Miralda-Escudé^{2,3}

¹*Harvard-Smithsonian Center for Astrophysics, Harvard University, 60 Garden Street, Cambridge, MA 02138*

²*Institució Catalana de Recerca i Estudis Avançats, Barcelona, Catalonia and*

³*Institut de Ciències del Cosmos, Universitat de Barcelona / IEEC, Barcelona, Catalonia*

Measurements of the baryonic acoustic oscillation (BAO) peak in the redshift-space correlation function yield the angular diameter distance $D_A(z)$ and the Hubble parameter $H(z)$ as a function of redshift, constraining the properties of dark energy and space curvature. We discuss the perturbations introduced in the galaxy correlation function by gravitational lensing through the effect of magnification bias and its cross-correlation with the galaxy density. At the BAO scale, gravitational lensing adds a small and slowly varying component to the galaxy correlation function and does not change its *shape* significantly, through which the BAO peak is measured. The relative shift in the position of the BAO peak caused by gravitational lensing in the angle-averaged correlation function is 10^{-4} at $z = 1$, rising to 10^{-3} at $z = 2.5$. Lensing effects are stronger near the line-of-sight, however the relative peak shift increases only to $10^{-3.3}$ and $10^{-2.4}$ at $z = 1$ and $z = 2.5$, when the galaxy correlation is averaged within 5 degrees of the line-of-sight (containing only 0.4% of the galaxy pairs in a survey). Furthermore, the lensing contribution can be measured separately and subtracted from the observed correlation at the BAO scale.

PACS numbers: 98.80.-k, 98.65.-r, 98.80.Jk, 98.62.Py

I. INTRODUCTION

A fundamental probe to the nature of the accelerated expansion of the universe is the comoving distance corresponding to a redshift interval, $d\chi = dz/H(z)$, where $H(z)$ is the Hubble constant at redshift z . The integrated function is related to the angular diameter distance, $D_A(z) = \chi(z)/(1+z)$ for a flat model. Deviations from this relation between $d\chi/dz$ and $D_A(z)$ are a probe to space curvature, so far consistent with zero [1]. Recently, particular attention is being paid to baryonic acoustic oscillations (BAO) in galaxy two-point statistics, as they provide a known physical scale tied to the sound horizon at the baryon decoupling epoch. Measurements of the BAO scale in the galaxy correlation function can be used to infer both $H(z)$ and $D_A(z)$ (see, e.g., [2–8] and see also, [9] for their sensitivity to cosmological parameters).

Gravitational lensing introduces perturbations on the galaxy correlation function by deflecting light rays from galaxies (see, e.g., [10–12]). The main effect arises from the lensing magnification of the sky area and the flux of each galaxy, known as magnification bias [13, 14]. This results in additional contributions to the observed galaxy correlation as a function of separation in redshift-space [15–17]. Another effect, which we shall not consider here, is the smoothing of the BAO peak caused by changes in the observed angular separation of galaxy pairs due to the lensing deflection, which induces a negligibly small shift on the position of the BAO peak (e.g., [16]).

We examine the modifications of the observed galaxy two-point correlation function $\xi_{\text{obs}}(\sigma, \pi)$ in redshift-space due to gravitational lensing, where $\sigma = D_A(z)(1+z)\phi$ and $\pi = \Delta z/H(z)$ are the comoving separations of galaxy pairs across

and along the line-of-sight in redshift-space, and ϕ and Δz are the observable angular and redshift separations. We evaluate the magnitude of the lensing contribution to clarify the level of accuracy at which the gravitational lensing effect needs to be taken into account for precision measurements of the BAO scale. We show that despite previous claims to the contrary Hui, Gaztanaga, and LoVerde [18] the effect of gravitational lensing is generally small for currently planned surveys, because gravitational lensing hardly changes the correlation function shape at the BAO scale and in practice galaxy pairs are averaged over a finite angular bin. We adopt a flat Λ CDM cosmology with $\Omega_m = 0.28$ and $H_0 = 70 \text{ km s}^{-1} \text{ Mpc}^{-1}$, according to recent measurements of the cosmic microwave background [1]. We set the speed of light $c \equiv 1$.

II. FORMALISM

We first summarize the basic equations for computing galaxy two-point correlation functions. In the linear approximation, the intrinsic galaxy correlation function is $\xi_{gg}(r) = b^2 \xi_{mm}(r)$, where b is a constant linear bias factor and $\xi_{mm}(r)$ is the mass correlation function. The redshift-space galaxy correlation function is computed by Fourier transforming the linearly biased matter power spectrum $b^2 P_{mm}(k)$ with the redshift-space enhancement factor arising from peculiar velocities [19],

$$\xi_{zz}(\sigma, \pi) = \int \frac{d^3 \mathbf{k}}{(2\pi)^3} e^{i\mathbf{k} \cdot \mathbf{s}} b^2 P_{mm}(k) (1 + \beta \mu_k^2)^2, \quad (1)$$

where $\mathbf{s} = (\sigma, \pi)$, $\mu_k = k_z/k$, $\beta = f/b$, $f = d \ln D / d \ln a$, and $D(z)$ is a growth factor of the matter density. We use the Smith et al. [20] approximation for computing the non-linear $\xi_{mm}(r)$ and $P_{mm}(k)$.

Lensing introduces two terms in the correlation function of galaxies above some luminosity L . The first is due to the auto-

*jyoo@cfa.harvard.edu

correlation of the magnification bias on two sources at z_1 and z_2 ($z_1 < z_2$),

$$\xi_{ll}(\sigma) = (3H_0^2\Omega_m\alpha)^2 \int_0^{\chi_1} d\chi \left[\frac{\chi(\chi_1 - \chi)}{a(\chi)\chi_1} \right]^2 w_p(\chi\phi), \quad (2)$$

where $\alpha = -d\log\bar{n}_g/d\log L - 1$, and $\bar{n}_g(L, \bar{z})$ is the cumulative number density of galaxies with luminosity above L at the mean source redshift \bar{z} . We assume the two sources are at nearly the same redshift, with a separation $\pi \ll \chi_1$. The dependence of the magnification bias on α arises from the combination of the magnification of the sky area and the flux amplification of the sources (see [13, 21]). The projected mass correlation function is

$$w_p(\sigma) = \int_{-\infty}^{\infty} d\pi \xi_{mm}(r = \sqrt{\sigma^2 + \pi^2}). \quad (3)$$

The other term that is added to the observed galaxy correlation is due to the cross-correlation of the intrinsic galaxy fluctuation and the magnification bias. Since the matter fluctuation along the line-of-sight is responsible for the magnification bias in the background galaxy, it correlates with the galaxy fluctuation and this cross-correlation is

$$\xi_{gl}(\sigma, \pi) = 3H_0^2\Omega_m\alpha \left[\int_0^{\chi_2} d\chi \frac{\chi(\chi_2 - \chi)}{a(\chi)\chi_2} \xi_{gm}(r_1) + (1 \leftrightarrow 2) \right], \quad (4)$$

where $r_1 = \sqrt{\phi^2\chi_1^2 + (\chi_1 - \chi)^2}$, $r_2 = \sqrt{\phi^2\chi^2 + (\chi_2 - \chi)^2}$, $\bar{\chi} = (\chi_1 + \chi_2)/2$, $\sigma = \phi\bar{\chi}$, $\pi = \chi_2 - \chi_1$, the galaxy-mass cross-correlation is $\xi_{gm}(r) = bc_{gm}\xi_{mm}(r)$, and c_{gm} is a galaxy-mass cross-correlation coefficient (e.g., [22]). The two added terms exchanging the subindexes (1,2) account for the effect of magnification bias in the background and foreground galaxy, respectively. After some rearrangement, we obtain, in the approximation $\pi \ll \bar{\chi}$,

$$\xi_{gl}(\sigma, \pi) = 3H_0^2\Omega_m\alpha(1 + \bar{z}) \times \left[\pi w_{p,gm}(\sigma) + 2 \int_{\pi}^{\infty} d\tau (\tau - \pi) \xi_{gm}(r) \right], \quad (5)$$

where $w_{p,gm}$ is the same projected correlation function as in Eq. (3) for ξ_{gm} , and $r = \sqrt{\sigma^2 + \tau^2}$. Equation (5) has been derived before without the inclusion of the second term (e.g., [23]), an approximation that is valid only when $\sigma \ll \pi$, in addition to $\pi \ll \bar{\chi}$. This second term is important for determining the functional shape of ξ_{gl} over all the redshift space, but is small in the region where the lensing effect is strongest, at $\sigma \ll \pi$. For the results presented here, we use the more exact Eq. (4) for computing ξ_{gl} . The total, observed galaxy correlation function is $\xi_{\text{obs}}(\sigma, \pi) = \xi_{zz}(\sigma, \pi) + \xi_{ll}(\sigma) + \xi_{gl}(\sigma, \pi)$.

III. RESULTS

Figure 1 shows the two-point correlation functions in redshift-space at $\bar{z} = 0.35$. The upper panels show the intrinsic galaxy correlation function ξ_{gg} (left) and the observed

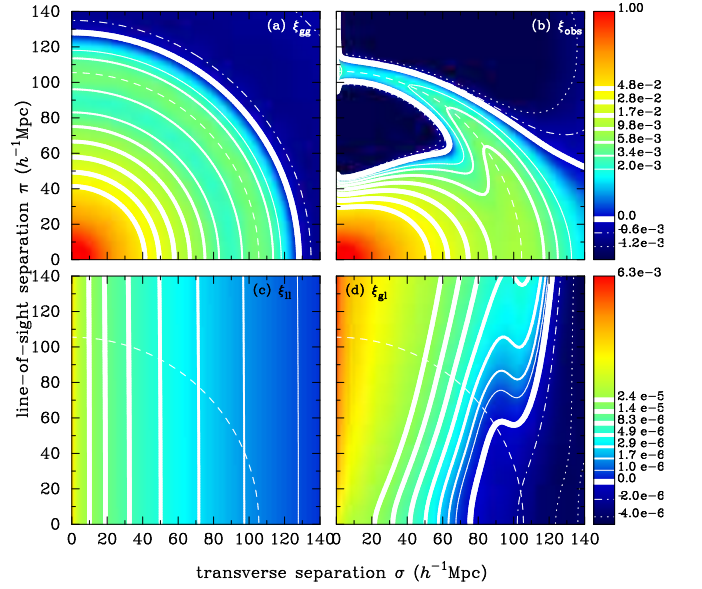


FIG. 1: (color online) Two-point correlation functions in redshift-space at $\bar{z} = 0.35$. (a) Intrinsic galaxy correlation function ξ_{gg} . (b) Observed galaxy correlation function $\xi_{\text{obs}} = \xi_{zz} + \xi_{ll} + \xi_{gl}$. (c) Magnification bias correlation function ξ_{ll} . (d) Cross-correlation function ξ_{gl} of the intrinsic galaxy fluctuation and the magnification bias. The color scale is proportional to the logarithm of the correlation function at $\xi \geq 1 \times 10^{-4}$ in the top panels, and at $\xi \geq 8 \times 10^{-7}$ in the bottom panels, below which the scale is linear with ξ . White contours of different thickness are as indicated in the right bars, with the thickest contour corresponding to $\xi = 0$. Negative contours are shown as dot-dashed and dotted curves. Since the lensing effect is small, the redshift-space correlation function ξ_{zz} is similar to ξ_{obs} in Panel (b), except for the small spot produced near $\sigma = 0$, $\pi = r_{\text{BAO}}$. A galaxy bias factor $b = 2$ and luminosity function slope $\alpha = 2$ are assumed. The baryonic acoustic oscillation scale r_{BAO} is shown as a dashed circle for reference.

galaxy correlation function ξ_{obs} (right). We choose a galaxy bias $b = 2$ at $\bar{z} = 0.35$ and a cross-correlation coefficient $c_{gm} = 1$, as measurements suggest for Sloan Digital Sky Survey (SDSS) luminous red galaxy (LRG) samples (see, e.g., [3, 8, 24]). The galaxy bias at other redshifts is computed assuming galaxies move as test particles responding to gravity in the linear regime, in which case $b(z) - 1 = [b(z = 0) - 1]/D(z)$, where $D(z)$ is the growth factor normalized to unity at $z = 0$ [26]. Note that ξ_{gg} scales as b^2 , and ξ_{obs} has an additional change of its contours with bias through the β parameter.

The BAO scale is defined as the distance traveled by a sound wave up to the baryon decoupling (drag) epoch at time t_d , $r_{\text{BAO}} = \int_0^{t_d} c_s (1 + z) dt = 155$ Mpc, where $c_s^2 = 1/3(1 + R)$, R is the baryon-photon ratio, and we use the [27] fitting formula for computing t_d (see also, [1, 28]). We indicate the BAO scale as a short-dash circle in Fig. 1. The bump in the correlation function at this scale shown by the contours of ξ_{obs} is the signature to be used to measure $r_{\text{BAO}}/D_A(z)$ and $r_{\text{BAO}}H(z)$. The redshift-space distortion squashes the contours of ξ_{obs} along the line-of-sight and changes the shape

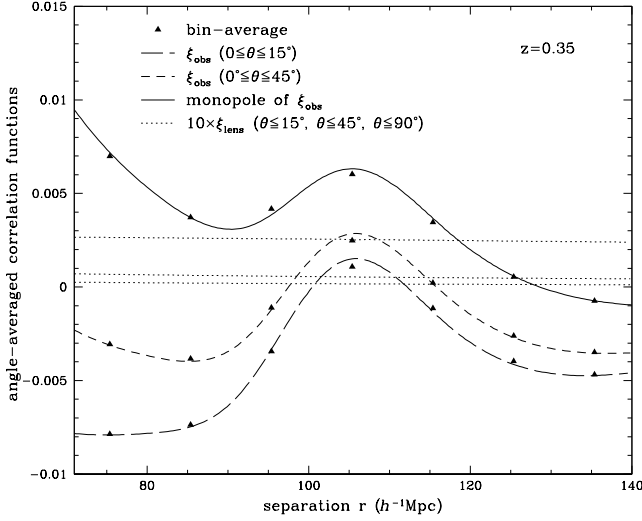


FIG. 2: Angle-averaged correlation functions and lensing contributions at $\bar{z} = 0.35$. Observed correlation function $\xi_{\text{obs}}(\sigma, \pi)$ is averaged over $0 \leq \theta < 15^\circ$ (long dashed), $0 \leq \theta < 45^\circ$ (short dashed), and over all angles (solid, monopole). Lensing contribution ($\xi_{\text{lens}} = \xi_{ll} + \xi_{gl}$) is shown multiplied by 10 and averaged over the same angular intervals (dotted, from top to bottom). Triangles show ξ_{obs} averaged over each radial bin of width $10h^{-1}$ Mpc.

of the BAO peak at each angle in the σ - π plane. The lensing effect is very small, and so the contours of ξ_{obs} in Fig. 1 are nearly identical to the contours of ξ_{zz} , except for a slight difference very close to the line-of-sight ($\sigma \ll \pi$), where the lensing effect is strongest.

The bottom panels show the correlation of the magnification bias ξ_{ll} (left) and the cross-correlation of the magnification bias and the intrinsic galaxy fluctuation ξ_{gl} (right). We use $\alpha = 2$ for the magnification bias, which is approximately the value for an LRG sample with $L > 3L_*$, close to the threshold for the SDSS [3, 29]. Note that the contour scale is smaller by a factor 100 than that in the upper panels. The function ξ_{ll} decreases with σ and depends very weakly on π through $\chi_1 = \bar{\chi} - \pi/2$ in Eq. (2), whereas ξ_{gl} decreases with σ and increases with π . The correlation ξ_{gl} contains a weak BAO ripple when σ is near the BAO scale, arising from the integration in Eq. (3) when the edge of the BAO sphere is seen in projection along the line-of-sight. The lensing correlations are of course largest near the line-of-sight at $\sigma \ll r_{\text{BAO}}$, where the BAO peak of ξ_{gl} is washed out by the integration.

Figure 2 shows $\xi_{\text{obs}}(r)$ and $\xi_{\text{lens}}(r) = \xi_{ll}(r) + \xi_{gl}(r)$ at $\bar{z} = 0.35$, averaged over volume with different angular intervals. The solid line is the monopole of ξ_{obs} . The short dashed and long dashed lines show ξ_{obs} averaged only over the angles $\theta < 45^\circ$ and $\theta < 15^\circ$ from the line-of-sight, respectively. The lensing contributions are indicated by the three dotted lines, averaged over the same angle intervals, from bottom to top; these curves are multiplied by 10 to enable visualization. Even within the narrow interval $\theta < 15^\circ$ (which contains only 3.4% of the galaxy pairs), the lensing contribution to ξ_{obs} is

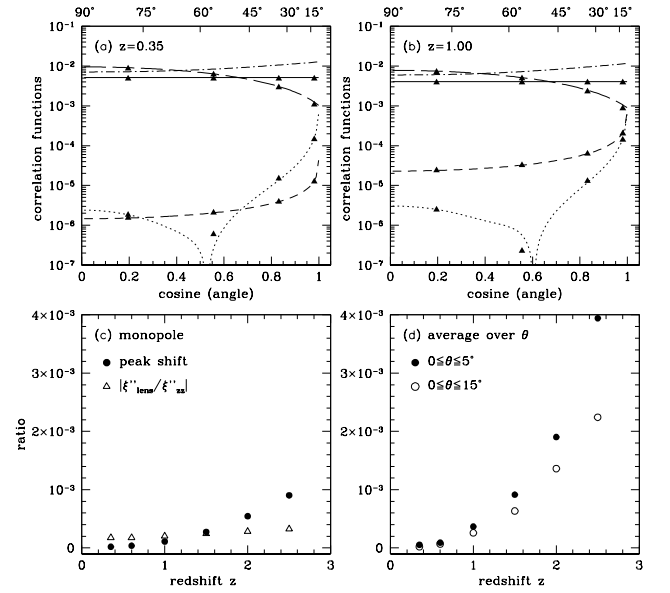


FIG. 3: Gravitational lensing effect on the correlation function at the BAO scale. Upper panels: Intrinsic galaxy correlation (ξ_{gg} , solid), redshift-space correlation (ξ_{zz} , long dashed), magnification bias correlation (ξ_{ll} , short dashed), and galaxy-magnification cross-correlation (ξ_{gl} , dotted) as a function of cosine angle $\mu = \cos \theta$. Note $\xi_{gl} < 0$ at $\mu \lesssim 0.6$, where its absolute value is plotted. Additional dot dashed curves show the BAO peak height $\Delta\xi_{\text{BAO}}$, defined in Eq. (6). Triangles show correlation functions averaged over radial width $10h^{-1}$ Mpc and angular width 22.5° . Bottom panels: As a function of redshift, circles and triangles represent lensing contribution to BAO peak position shift and height (Eqs. (7) and (6)) averaged over all angles (left), and filled and empty circles show lensing contributions to BAO peak position shift averaged over angles within 5 and 15 degrees (right). We compute ξ_{ll} and ξ_{gl} at $\mu \leq 0.9999$ (corresponding to $\sigma = 1.5h^{-1}$ Mpc at $r = r_{\text{BAO}}$), beyond which the linear bias approximation may be inaccurate (cf. Fig. 4).

$\sim 3 \times 10^{-4}$, while the contrast of the BAO peak is $\Delta\xi \sim 0.01$. Note that the lensing contribution is dominated by ξ_{gl} , and therefore it scales as αbc_{gm} . The lensing effect adds only a small component to ξ_{obs} that is very slowly varying with r , and cannot alter the shape of the BAO peak in any appreciable way. Vallinotto et al. [16] also reached the same conclusion that the magnification bias on the BAO peak shift is negligible, although they compared the intrinsic galaxy correlation function ξ_{gg} with the lensing contribution in the transverse direction ($\pi = 0, \sigma \simeq r_{\text{BAO}}$).

Figure 3 examines the gravitational lensing effect at the BAO scale, $r = r_{\text{BAO}}$, as a function of the cosine angle $\mu = \cos \theta = \pi/r$. Note that an equal amount of volume is available to measure the correlation function per interval $d\mu$. The upper panels show ξ_{gg} (solid), ξ_{zz} (long dashed), ξ_{ll} (short dashed), and ξ_{gl} (dotted), at $\bar{z} = 0.35$ and $\bar{z} = 1$, with galaxy bias factor $b = 2$ and $b = 2.3$, respectively. A fifth curve (dot dashed) shows the BAO peak amplitude $\Delta\xi_{\text{BAO}}$, which we define in the next paragraph. All the functions are evaluated at $r = r_{\text{BAO}}$. The slope of the luminosity function

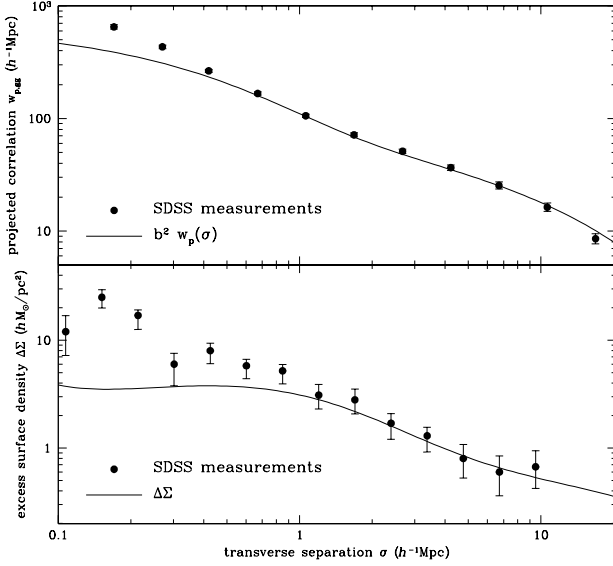


FIG. 4: Projected galaxy correlation $w_{p,gg}$ and excess surface density $\Delta\Sigma$ computed from the non-linear mass correlation function ξ_{mm} (solid), compared with projected galaxy correlation and lensing shear measurements from SDSS [24, 25]. This validates our modeling of lensing effects based on linear bias for $\sigma \geq 1h^{-1}$ Mpc.

is fixed to $\alpha = 2$. Triangles show the averaged correlation function over angular bins of width $\Delta r = 10h^{-1}$ Mpc and $\Delta\theta = 22.5^\circ$.

To understand the effect of lensing on the BAO peak, one should note that the ability to measure the peak position r_{BAO} depends on the *shape* and *height* of the BAO peak, rather than the specific value of ξ_{obs} at r_{BAO} . For example, near the line of sight ($\mu = 1$), the redshift-space correlation function $\xi_{zz}(\simeq \xi_{\text{obs}})$ happens to be very close to zero at $r = r_{\text{BAO}}$, so a small lensing contribution can change $\xi_{\text{obs}}(r_{\text{BAO}})$ by an increased factor. However, this is totally irrelevant for measuring the BAO peak position and for quantifying the importance of lensing. We therefore choose a definition of the BAO peak height $\Delta\xi_{\text{BAO}}$ in terms of the second derivative of ξ_{zz} at r_{BAO} :

$$\Delta\xi_{\text{BAO}}(\theta) = -\frac{\sigma_{\text{BAO}}^2}{2} \xi_{zz}''(r_{\text{BAO}}, \theta), \quad (6)$$

where the prime indicates a partial derivative with respect to r at fixed angle θ , and σ_{BAO} is a constant that represents the width of the BAO peak and can be adjusted to fit the peak height, $\Delta\xi_{\text{BAO}}$. This definition is exact when ξ_{zz} is approximated as a linear component plus a Gaussian bump of width $\sigma_{\text{BAO}}/\sqrt{2}$ at $r = r_{\text{BAO}}$. We choose $\sigma_{\text{BAO}} = 15h^{-1}$ Mpc, which results in the dot dashed curves shown in Fig. 3. We see that $\Delta\xi_{\text{BAO}}(\mu)$ increases slightly with μ , in contrast to $\xi_{zz}(\mu)$ which drops sharply with μ close to $\mu = 1$ (the width of the BAO peak is actually narrower at $\mu \simeq 1$ than for the monopole, so $\Delta\xi_{\text{BAO}}$ increases less with μ if this is taken into account). This indicates that Eq. (6) remains a very good approximation, as ξ_{zz} has negligible curvature around the BAO

scale once the Gaussian component is removed.

The ratio $\xi_{\text{lens}}/\Delta\xi_{\text{BAO}}$ is $\lesssim 10^{-2.5}$ over most of the volume at $\bar{z} < 1$, and is $\sim 2\%$ at $\theta \leq 15^\circ$. At $\bar{z} > 1$, the ξ_{ll} lensing contribution becomes dominant and increases roughly as $\bar{\chi}^3$. Since the lensing contribution to ξ_{obs} has a very slow variation with r , the effect on the measurement of the BAO scale is much smaller than $\xi_{\text{lens}}/\Delta\xi_{\text{BAO}}$. The radial shift $\Delta r_{\text{max}} = r_{\text{BAO}} - r_{\text{obs}}$ in the maximum of the correlation function at fixed θ is

$$\frac{\Delta r_{\text{max}}}{r_{\text{BAO}}} = -\frac{\xi'_{\text{lens}}}{2\Delta\xi_{\text{BAO}}} \frac{\sigma_{\text{BAO}}^2}{r_{\text{BAO}}}. \quad (7)$$

Note that the shift Δr_{max} in Eq. (7) is independent of our choice of the σ_{BAO} value. The bottom panels of Fig. 3 show this relative radial peak shift (circle), and the relative change in the BAO peak height, $|\xi''_{\text{lens}}/\xi''_{zz}|$ (triangle), for the angle-averaged case (left), and averaging over $\theta \leq 5^\circ$ (right). The peak shift $\Delta r_{\text{max}}/r_{\text{BAO}}$ is, for the angle-averaged case, $\sim 10^{-4}$ at $\bar{z} \leq 1$, rising to $\sim 10^{-3}$ at $z = 2.5$. When restricted to the narrow region near the line-of-sight $\theta \leq 5^\circ$, this peak shift increases by a factor of only ~ 4 , still remaining a very small effect. We have checked that even at 1° from the line-of-sight the peak shift due to lensing grows only by another factor of 2 compared to the $\theta \leq 5^\circ$ case.

Naturally, in any galaxy survey, the error to which the BAO peak position can be measured in a region within an angle θ of the line-of-sight is increased by at least the factor $\sqrt{2}/\theta$ compared to the angle-averaged measurement, owing to the increased shot noise and sampling variance. For the purpose of measuring the radial BAO peak position, the galaxy correlation function always needs to be averaged over a finite angular bin, and no substantial added precision is obtained for very small angles from the line-of-sight. Therefore, lensing effects on the BAO peak position will always be very small in practice. The lensing contribution to the BAO height is $\sim 2 \times 10^{-4}$ for the monopole, increasing very slowly with redshift, and is actually smaller near the line-of-sight. This shows that even though the value of ξ_{lens} at r_{BAO} is largest near the line-of-sight, its effect on the BAO peak is not necessarily so, because adding a constant to the correlation function is irrelevant for measuring the BAO peak.

The impact of gravitational lensing on the BAO peak was previously discussed by Hui et al. [18]. We disagree with their conclusion that there are large lensing effects. Hui et al. [18] define a fractional change in the BAO peak height as $(\xi_{\text{obs}} - \xi_{gg})/\xi_{gg}$. As discussed above, this quantity is irrelevant because adding a constant to the correlation function has no effect on the measurement of the BAO peak. Moreover, the value of ξ_{gg} at the BAO peak, or of ξ_{zz} when the correlation is measured in redshift space over a specific angular range, may happen to be near zero, which may give rise to a large fractional change of ξ_{gg} due to the lensing effect, but this is equally irrelevant: only the amplitude of the BAO peak matters, and not the value of ξ at the peak.

Hui et al. [18] also claim that lensing has strong effects in

the line-of-sight direction.¹ In reality, the correlation function can only be observed averaged within a finite angle of the line-of-sight, and can only be computed using a constant bias down to some minimum separation for which the linear bias approximation for the projected galaxy-mass cross-correlation is reasonable. This explains why Hui et al. [18] find a shift in the BAO peak location on the line-of-sight direction of 3% that is nearly redshift independent (see their Fig. 8a; our values of bias and slope correspond to $(5s-2)/b = 2$ in their notation), whereas we find that within 5 degrees of the line-of-sight the shift increases rapidly with redshift and reaches only 0.4% at $z = 2.5$, and within 1 degree of the line-of-sight the shift is larger by only a factor ~ 2 . For the angle-averaged lensing effect, we also disagree with the results of Hui et al. [18]: they find a peak shift of 0.4% at $z=2.5$ (for the same bias and slope we use), compared to our result of 0.1%.

We note that if one insists on measuring the correlation of galaxies exactly on the line-of-sight, strong lensing occurs and the background galaxy is imaged into an Einstein ring, an effect that is already detected (see, e.g., the Sloan Lenses ACS Survey [30]). However, this lensing effect has no special feature at the BAO scale and has no interesting effect on the ability to measure the BAO peak in the galaxy correlation function.

Finally, we comment on the way to observationally separate the lensing contribution from ξ_{obs} . Considering galaxies of two types with bias factors b_1 and b_2 and luminosity function slopes α_1 and α_2 , the parity of the correlation functions $\xi_{\text{obs}}(\sigma, \pi)$ is even under a change of sign of π , except for the galaxy-magnification cross-correlation ξ_{gl} , which is different depending on the galaxy type that is in the foreground or background. For simplicity, we consider the case $\sigma \ll \pi$, when the second term in Eq. (5) can be neglected. Hence, the asymmetry of the cross-correlation function of two different types of galaxies yields the galaxy-lensing contribution:

$$\begin{aligned} \xi_{\text{obs}}(\sigma, \pi) - \xi_{\text{obs}}(\sigma, -\pi) &= \xi_{gl}(z_1 < z_2) - \xi_{gl}(z_2 < z_1) \\ &= (b_1\alpha_2 - b_2\alpha_1) 3H_0^2\Omega_m (1 + \bar{z}) \pi w_p(\sigma). \end{aligned} \quad (8)$$

Consequently, it is in principle possible to directly separate the ξ_{gl} contribution at the BAO scale purely from observations. Alternatively, since the lensing contribution is very small at the BAO scale, one can measure ξ_{gl} at large π (e.g., [21]), where the contribution from ξ_{zz} is small, and use the known dependence on π to subtract its contribution from the measurements of ξ_{obs} at the BAO scale.

IV. DISCUSSION

We have shown that modifications of the galaxy correlation function caused by gravitational lensing are a tiny effect for the purpose of measuring the BAO scale. The lensing contribution to the correlation function near the BAO peak is $\xi_{\text{lens}} \sim 10^{-4}$ at $\bar{z} < 1$, even within 15° of the line-of-sight. Moreover, the lensing contribution is nearly constant as a function of radius, so the ability to measure the BAO peak and its shape in any galaxy survey is not affected. The galaxy correlation function is averaged over a finite angular bin, further suppressing the lensing effect. The shift in the position of the BAO peak due to lensing in the angle-averaged correlation function is less than 1 part in 10^4 at $\bar{z} \leq 1$ and it increases to $\sim 10^{-3}$ at $\bar{z} = 2.5$. This peak shift is increased by a factor of only 4 within 5 degrees of the line-of-sight, where just 0.4% of the galaxy pairs are available for measuring the correlation function. The lensing effect increases with the luminosity function slope α , but not sufficiently to make it substantial for any known population of sources.

As we discussed in Sec. III, when two types of galaxies are used to measure the correlation function, we can directly measure the lensing contribution ξ_{lens} from observations and subtract it before we estimate the BAO peak position. In general, the addition of any broadband power to the correlation function by known physical effects can be modeled and removed. The method for measuring the position of the BAO peak may be optimized to minimize the dependence on added broad-band power from several physical effects in addition to lensing [31, 32]. Therefore, the lensing effect we have computed here is likely to be further reduced when using optimized definitions of the BAO scale.

The linear bias approximation we have used here becomes invalid for computing the galaxy-magnification cross-correlation in Eq. (4) close to the line-of-sight, when the transverse separation σ is small. The bias coefficients b and c_{gm} may be scale-dependent, and other non-linear terms may become important. However, the correlations induced by lensing can be tested by independent observations of lensing effects around galaxies [24, 33, 34]. Figure 4 shows the projected galaxy correlation function $w_{p,gg}$ [25] and the excess surface density $\Delta\Sigma$ inferred from weak lensing measurements [24], for the SDSS main sample of galaxies. Also shown as solid lines are the result for w_p from the mass correlation function used in this paper and for the excess surface density,

$$\Delta\Sigma(\sigma) \propto \frac{2}{\sigma^2} \int_0^\sigma w_{p,gm}(R) R dR - w_{p,gm}(\sigma). \quad (9)$$

Normalization is adjusted to match the data on large scales. For other types of galaxies one can use the results of Sheldon et al. [24] to match the required value of bc_{gm} .

The measurements are in reasonable agreement with the linear bias approximation at $\sigma \geq 1h^{-1}\text{Mpc}$. At smaller separations, the shape of the galaxy-mass cross-correlation is clearly steeper than our simple model. This is not surprising because galaxies tend to occupy the central positions in halos. The mass auto-correlation function at these small scales reflects the density profiles of dark matter halos, which have a

¹ Hui et al. [18] calculate the line-of-sight galaxy-lensing correlation using the projected mass auto-correlation with a constant bias factor extrapolated to zero separation. This yields the average lensing convergence behind a random mass particle (times the assumed bias factor), instead of the convergence behind the center of a galaxy. In reality, whenever the lensing effect is observed exactly on the line-of-sight to a galaxy with a central cusp, strong lensing must occur.

slope that gradually flattens at small radius, whereas galaxies are more centrally concentrated than mass in halos (see, e.g., [35, 36] for the one-halo contributions). These small scales would affect the BAO signal at angles $\theta \lesssim 0.5^\circ$ for the SDSS main galaxy samples and $\theta \lesssim 1.0^\circ$ for the LRG samples (see, e.g., [33]), containing a very small fraction of the galaxy pairs. We conclude that non-linear effects can be neglected, except within angles as small as 1.0° , where they can be calibrated to the observational results.

Acknowledgments

We thank Adam Lidz, Daniel Eisenstein, David Weinberg, and Uroš Seljak for useful discussions. J. Y. is supported by the Harvard College Observatory under the Donald H. Menzel fund. J. M. is supported by the Spanish grants AYA2006-06341, AYA2006-15623-C02-01, AYA2009-09745 and MEC-CSD2007-00060.

-
- [1] E. Komatsu, J. Dunkley, M. R. Nolta, C. L. Bennett, B. Gold, G. Hinshaw, N. Jarosik, D. Larson, M. Limon, L. Page, et al., ArXiv e-prints (2008), 0803.0547.
 - [2] A. Albrecht et al., ArXiv Astrophysics e-prints (2006), astro-ph/0609591.
 - [3] D. J. Eisenstein, M. Blanton, I. Zehavi, N. Bahcall, J. Brinkmann, J. Loveday, A. Meiksin, and D. Schneider, *Astrophys. J.* **619**, 178 (2005), arXiv:astro-ph/0411559.
 - [4] T. Okumura, T. Matsubara, D. J. Eisenstein, I. Kayo, C. Hikage, A. S. Szalay, and D. P. Schneider, *Astrophys. J.* **676**, 889 (2008), arXiv:0711.3640.
 - [5] N. Padmanabhan et al., *Mon. Not. R. Astron. Soc.* **378**, 852 (2007), arXiv:astro-ph/0605302.
 - [6] W. J. Percival, R. C. Nichol, D. J. Eisenstein, D. H. Weinberg, M. Fukugita, A. C. Pope, D. P. Schneider, A. S. Szalay, M. S. Vogeley, I. Zehavi, et al., *Astrophys. J.* **657**, 51 (2007), arXiv:astro-ph/0608635.
 - [7] H.-J. Seo and D. J. Eisenstein, *Astrophys. J.* **598**, 720 (2003), arXiv:astro-ph/0307460.
 - [8] M. Tegmark et al., *Phys. Rev. D* **74**, 123507 (2006), arXiv:astro-ph/0608632.
 - [9] D. J. Eisenstein, *New Astronomy Review* **49**, 360 (2005).
 - [10] R. Blandford and R. Narayan, *Astrophys. J.* **310**, 568 (1986).
 - [11] J. E. Gunn, *Astrophys. J.* **150**, 737 (1967).
 - [12] N. Kaiser, *Astrophys. J.* **388**, 272 (1992).
 - [13] R. Narayan, *Astrophys. J. Lett.* **339**, L53 (1989).
 - [14] E. L. Turner, *Astrophys. J. Lett.* **242**, L135 (1980).
 - [15] T. Matsubara, *Astrophys. J. Lett.* **537**, L77 (2000), arXiv:astro-ph/0004392.
 - [16] A. Vallinotto, S. Dodelson, C. Schimd, and J.-P. Uzan, *Phys. Rev. D* **75**, 103509 (2007), arXiv:astro-ph/0702606.
 - [17] J. Yoo, *Phys. Rev. D* **79**, 023517 (2009), arXiv:0808.3138.
 - [18] L. Hui, E. Gaztanaga, and M. LoVerde, *Phys. Rev. D* **76**, 103502 (2007), astro-ph/0706.1071.
 - [19] N. Kaiser, *Mon. Not. R. Astron. Soc.* **227**, 1 (1987).
 - [20] R. E. Smith, J. A. Peacock, A. Jenkins, S. D. M. White, C. S. Frenk, F. R. Pearce, P. A. Thomas, G. Efstathiou, and H. M. P. Couchman, *Mon. Not. R. Astron. Soc.* **341**, 1311 (2003), arXiv:astro-ph/0207664.
 - [21] R. Scranton et al., *Astrophys. J.* **633**, 589 (2005), arXiv:astro-ph/0504510.
 - [22] U.-L. Pen, *Astrophys. J.* **504**, 601 (1998), astro-ph/9711180.
 - [23] M. Bartelmann, *Astron. Astrophys.* **298**, 661 (1995), arXiv:astro-ph/9407091.
 - [24] E. S. Sheldon et al., *Astron. J.* **127**, 2544 (2004), astro-ph/0312036.
 - [25] I. Zehavi and et al., *Astrophys. J.* **630**, 1 (2005), astro-ph/0408569.
 - [26] J. N. Fry, *Astrophys. J. Lett.* **461**, L65+ (1996).
 - [27] D. J. Eisenstein and W. Hu, *Astrophys. J.* **496**, 605 (1998), arXiv:astro-ph/9709112.
 - [28] W. Hu, in *Observing Dark Energy*, edited by S. C. Wolff and T. R. Lauer (2005), vol. 339 of *Astronomical Society of the Pacific Conference Series*, pp. 215+.
 - [29] R. J. Cool, D. J. Eisenstein, X. Fan, M. Fukugita, L. Jiang, C. Maraston, A. Meiksin, D. P. Schneider, and D. A. Wake, *Astrophys. J.* **682**, 919 (2008), 0804.4516.
 - [30] T. Treu, L. V. E. Koopmans, A. S. Bolton, S. Burles, and L. A. Moustakas, in *Bulletin of the American Astronomical Society* (2005), vol. 37 of *Bulletin of the American Astronomical Society*, pp. 1498+.
 - [31] H.-J. Seo, E. R. Siegel, D. J. Eisenstein, and M. White, *Astrophys. J.* **686**, 13 (2008), 0805.0117.
 - [32] X. Xu, M. White, N. Padmanabhan, D. Eisenstein, J. Eckel, K. Mehta, M. Metchnik, P. Pinto, and H. Seo, ArXiv e-prints (2010), 1001.2324.
 - [33] R. Mandelbaum, C. M. Hirata, U. Seljak, J. Guzik, N. Padmanabhan, C. Blake, M. R. Blanton, R. Lupton, and J. Brinkmann, *Mon. Not. R. Astron. Soc.* **361**, 1287 (2005), astro-ph/0501201.
 - [34] R. Mandelbaum, U. Seljak, R. J. Cool, M. Blanton, C. M. Hirata, and J. Brinkmann, *Mon. Not. R. Astron. Soc.* **372**, 758 (2006), astro-ph/0605476.
 - [35] J. Yoo, J. L. Tinker, D. H. Weinberg, Z. Zheng, N. Katz, and R. Davé, *Astrophys. J.* **652**, 26 (2006), astro-ph/0511580.
 - [36] I. Zehavi and et al., *Astrophys. J.* **608**, 16 (2004), astro-ph/0301280.